



DALHOUSIE UNIVERSITY

Retrieved from DalSpace, the institutional repository of
Dalhousie University

<https://dalspace.library.dal.ca/handle/10222/79711>

Version: Post-print

Publisher's version: Feng, Xibo; Otero de la Roza, Alberto; and Johnson, Erin. (2018). The effect of electronic excitation on London dispersion. *Canadian Journal of Chemistry*, 96, 730-73. <https://doi.org/10.1139/cjc-2017-0726>

1 **The effect of electronic excitation on London dispersion**

2 Xibo Feng,¹ Alberto Otero-de-la-Roza,² and Erin R. Johnson^{1, a)}

3 ¹⁾*Department of Chemistry, Dalhousie University, 6274 Coburg Rd,*
4 *P.O.Box 15000 B3H 4R2, Halifax, Nova Scotia, Canada*

5 ²⁾*Department of Chemistry, University of British Columbia,*
6 *Okanagan, 3247 University Way, Kelowna, British Columbia,*
7 *Canada V1V 1V7.*

8 (Dated: 14 January 2018)

^{a)}Electronic mail: erin.johnson@dal.ca; Telephone: 902-494-3409

9 **Abstract**

10 Atomic and molecular dispersion coefficients can now be calculated routinely using
11 density-functional theory. In this work, we present the first determination of how elec-
12 tronic excitation affects molecular C_6 London dispersion coefficients from the exchange-hole
13 dipole moment (XDM) dispersion model. Excited states are typically found to have larger
14 dispersion coefficients than the corresponding ground states, due to their more diffuse elec-
15 tron densities. A particular focus is both intramolecular and intermolecular charge-transfer
16 excitations, which have high absorbance intensities and are important in organic dyes, light-
17 emitting diodes, and photovoltaics. In these classes of molecules, the increase in C_6 for
18 the electron-accepting moiety is largely offset by a decrease in C_6 for the electron-donating
19 moiety. As result, the change in dispersion energy for a chromophore interacting with
20 neighbouring molecules in the condensed phase is minimal.

21 **Keywords:** London dispersion, excited states, density-functional theory

22 I. INTRODUCTION

23 The study of electronic excitations is essential in many areas of chemistry. Molecular elec-
24 tronic excitations play important roles in the design and fabrication of organic electronics^{1,2}
25 (sensors, light-emitting diodes, photovoltaics, etc.). While properties of the excited state
26 have been extensively studied for single molecules in the gas-phase and in solution, little is
27 known regarding how excitation of a single molecule affects the intermolecular interactions
28 with its neighbours.^{3,4} In particular, to our knowledge, there has only been one investigation
29 to date as to how electronic excitation affects the strength of intermolecular London dis-
30 persion interactions⁵ and this was limited to a small set of van der Waals complexes rather
31 than common chromophores.⁶ This may be, in part, because popular empirical dispersion
32 models have dispersion coefficients that are either fixed⁷ or depend only on the geometry⁸
33 and consequently cannot describe correctly the change in intermolecular dispersion during
34 a vertical excitation. Alternatively, while non-local density-functional dispersion models are
35 transferable to excited states,⁵ they do not directly provide atomic or molecular dispersion
36 coefficients.

37 The exchange-hole dipole moment (XDM) model⁹⁻¹¹, in the context of density-functional
38 theory (DFT), is uniquely suited to address the question of how electronic excitation af-
39 fects London dispersion. The XDM model provides a non-empirical means of calculating
40 accurate C_6 (and higher-order¹²) dispersion coefficients directly from the electron density.
41 As such, the XDM dispersion coefficients are sensitive to changes in an atom’s electronic
42 environment¹³⁻¹⁵ and the method is completely transferable, without modification, from
43 ground-state to excited-state electron densities.

44 In XDM, the dispersion energy is an *a posteriori* correction to the self-consistent energy,
45 calculated using one of the common density functionals. The dispersion energy is written
46 as a sum over all pairs of atoms, i and j separated by a distance R_{ij} , and includes C_6 , C_8 ,
47 and C_{10} dispersion terms.

$$E_{\text{disp}}^{\text{XDM}} = - \sum_{n=6,8,10} \sum_{i<j} \frac{C_{n,ij} f_n(R_{ij})}{R_{ij}^n} \quad (1)$$

48 The damping function, $f_n(R_{ij})$, prevents the divergence of the dispersion energy at small
49 internuclear separations. The atomic C_6 dispersion coefficients are determined from the

50 exchange-hole dipole moment integrals, $\langle d_X^2 \rangle$, and atom-in-molecule polarisabilities, α .

$$C_{6,ij} = \frac{\alpha_i \alpha_j \langle d_X^2 \rangle_i \langle d_X^2 \rangle_j}{\alpha_i \langle d_X^2 \rangle_j + \alpha_j \langle d_X^2 \rangle_i} \quad (2)$$

51 Analogous formulae can be written for the higher-order dispersion coefficients and involve
52 higher-order exchange-hole multipole moments. The moment integrals and polarisabilities
53 are both functions of the electron density and consequently vary with atomic environment.
54 Interested readers are directed to Ref. 11 for a comprehensive review of the XDM equations
55 and the theory underpinning the model. The overall molecular C_n dispersion coefficient can
56 be evaluated by summing over all atom pairs.

$$C_n = \sum_{ij} C_{n,ij} \quad (3)$$

57 This value is the C_n dispersion coefficient for the interaction between one molecule and a
58 second, identical molecule.

59 In this work, the XDM model is applied to investigate how the molecular dispersion
60 coefficients change upon electronic excitation for a small collection of molecular systems,
61 which can be broken down into three classes. These are $\pi \rightarrow \pi^*$ excitations in conjugated
62 hydrocarbons, charge-transfer excitations in push-pull chromophores of 4,4'-disubstituted
63 biphenyls, and intermolecular excitations in charge-transfer complexes. Additionally, we
64 consider a set of ten molecular crystals and co-crystals and assess how changes in dispersion
65 coefficients resulting from electronic excitation affect the dispersion energy for interaction
66 of a single excited molecule with the surrounding bulk. This dispersion contribution to the
67 excitation energy has not previously been considered when modeling electronic excitations
68 of molecules in the condensed phase.

69 II. COMPUTATIONAL METHODS

70 A. Molecular calculations

71 All molecular calculations were performed using the Gaussian 09 program.¹⁶ Geome-
72 tries of all molecules and intermolecular complexes were optimized using B3LYP^{17,18} or
73 B3LYP-XDM, respectively, both with the 6-31+G* basis set. Subsequent single-point en-

74 ergy calculations and time-dependent density-functional theory (TD-DFT)^{19–22} calculations
 75 were performed with either the 6-31+G* basis set for single molecules or aug-cc-pVDZ for
 76 complexes and either the B3LYP^{17,18} or CAM-B3LYP²³ density functionals. Usually the first
 77 singlet excited state was considered, but occasionally a higher excited state was investigated,
 78 corresponding to the charge-transfer state for the push-pull chromophores or intermolecular
 79 charge-transfer complexes (see below).

80 Change-transfer excitations are well known to be problematic for functionals with little
 81 or no exact-exchange mixing,^{24–30} due to the density-functional “delocalisation” or “charge-
 82 transfer” error.^{31–36} As such, calculations on intermolecular charge-transfer complexes were
 83 performed using systematic series of hybrid and range-separated hybrid density function-
 84 als with varying exact-exchange mixing. Specifically, a family of BLYP^{18,37}-based hybrid
 85 functionals of the form

$$E_{XC} = a_X E_X^{\text{exact}} + (1 - a_X) E_X^{\text{B88}} + E_C^{\text{LYP}} \quad (4)$$

86 was used, where the exact-exchange mixing fraction, a_X was varied from 0 to 1 in increments
 87 of 0.1. Similarly, we also considered a family of range-separated hybrid functionals based
 88 on LC-BLYP.³⁸ In these functionals, the interelectronic Coulomb potential is divided into
 89 short- and long-range terms using the error function:

$$\frac{1}{r_{12}} = \frac{1 - \text{erf}(\omega r_{12})}{r_{12}} + \frac{\text{erf}(\omega r_{12})}{r_{12}}. \quad (5)$$

90 This modified Coulomb potential is then used in evaluation of the exchange energy such
 91 that the short-range portion is treated with the B88 generalised-gradient-approximation
 92 functional³⁷ and the long-range component is treated with exact exchange. The length of
 93 this range-separation is determined by the parameter ω , whose value was varied from 0 to
 94 1 Bohr⁻¹ in increments of 0.1 Bohr⁻¹.

95 In evaluation of the exchange-hole dipole moments, and resulting XDM dispersion co-
 96 efficients, the Becke-Roussel exchange-hole model³⁹ was used in all calculations. As such,
 97 the full two-particle density matrix for the excited state was not required. We need only
 98 the expansion of the Kohn-Sham orbitals in terms of the atomic basis functions, which
 99 can be obtained from the wavefunction file. The “density=current” option in the Gaussian

100 program¹⁶ was used to generate wavefunction files for excited states. The ground state den-
 101 sity, ρ_{gs} , is obtained from the usual sum of the squares of the occupied, real Kohn-Sham
 102 orbitals: $\rho_{gs} = \sum_{i,\sigma} \psi_{i\sigma}^2(\mathbf{r})$. The excited-state density, ρ_{ex} is determined from the first-order
 103 density response and is given by^{40,41}

$$\rho_{ex} = \rho_{gs} + \sum_{i,a,\sigma} P_{ia\sigma} \psi_{i\sigma}(\mathbf{r}) \psi_{a\sigma}(\mathbf{r}), \quad (6)$$

104 where index i refers to the occupied Kohn-Sham orbitals, index a the virtual Kohn-Sham
 105 orbitals, and σ denotes the electron spin. The $P_{ia\sigma}$ coefficients are determined from solution
 106 of the Casida equation in TD-DFT.^{19,42} The BR procedure is then applied to calculate
 107 the exchange-hole dipole moments and dispersion coefficients^{10,11,43} from the density and
 108 orbitals. The postg program⁴⁴ was used to calculate the C_6 dispersion coefficients and
 109 Hirshfeld⁴⁵ atomic charges for both the ground and excited states.

110 B. Solid-state calculations

111 Crystal structures of 4-amino-4'-nitrobiphenyl, A3MN [2-Amino-3-((E)-(4-(diethylamino)
 112 benzyldene)amino)maleonitrile],⁴⁶ coumarin, 6-aminocoumarin, and the benzene/hexafluoro-
 113 benzene, N,N-dimethylaniline/hexafluorobenzene, naphthalene/hexafluorobenzene, tetra-
 114 cyanoethylene/naphthalene, chloranilic acid/pyrazine, and 2,5-dimethylbenzoquinone/bis-
 115 (hydroquinone) co-crystals, were obtained from the Cambridge Crystallographic Data
 116 Centre⁴⁷ (codes: KEFLEM01, PAQMIE01, RAZLEK, BEZZAJ, BICVUE01, DMAFBZ01,
 117 IVOBOK, CYENAP, BOQHOE, and CISCOW, respectively). The structures of these crys-
 118 tals (both atomic positions and unit-cell parameters) were then optimized with B86bPBE-
 119 XDM^{11,48-50} using the Quantum ESPRESSO program.⁵¹ These calculations used Projector-
 120 Augmented-Wave (PAW) pseudopotentials, a $4 \times 4 \times 4$ k-point mesh, and energy and density
 121 plane-wave cut-offs of 60 and 600 Ry, respectively. After optimization, single-point energy
 122 and TD-DFT calculations were performed on a single molecule cut from the crystal at this
 123 fixed geometry. These calculations used Gaussian 09 as detailed above, with the B3LYP
 124 functional and the 6-31+G* basis set. The London dispersion coefficients were calculated
 125 from the resulting electron densities using the postg program.⁴⁴ These coefficients were then
 126 used to evaluate the dispersion energy for interaction of this single molecule, in either its

127 ground or excited state, with the remainder of the crystal, using the critic2 program.⁵²

128 III. RESULTS AND DISCUSSION

129 A. Conjugated hydrocarbons

130 We begin by considering the $\pi \rightarrow \pi^*$ excitations for the set of conjugated hydrocar-
131 bon molecules shown in Figure 1. This set consists of a mixture of straight-chain alkenes,
132 biphenyls, and stilbenes. As $\pi \rightarrow \pi^*$ excitations are much less sensitive to the choice of
133 DFT method than are charge-transfer excitations, we consider only B3LYP results. Fig-
134 ure 2 shows the percent change in molecular C_6 dispersion coefficients for all members of
135 this set, as a function of either excitation energy (a,b) or chain length (c,d).

136 The results in Figure 2(a,b) show that the percent change in molecular C_6 upon exci-
137 tation increases exponentially with increasing excitation energy for each distinct series of
138 compounds (alkenes, stilbenes, and biphenyls). This is to be expected as the valence electron
139 becomes more weakly bound in higher-energy excited states, causing the electron density
140 to be more diffuse, which in turn causes the dispersion coefficients to increase. In partic-
141 ular the percent increase in C_6 upon excitation of ethylene is extremely large (in excess of
142 200%) and even larger increases appear in high-energy Rydberg excitations. However, as
143 such high-energy excitations are not observed in everyday chemical applications, we focus
144 our attention on lower-energy $\pi \rightarrow \pi^*$ and charge-transfer excitations.

145 While the excitation energies for the conjugated-chain set vary significantly depending
146 on the molecule type, a simplified picture of the effect of excitation on C_6 can be obtained
147 by recourse to a particle-in-a-box model in which only the chain length of each hydrocarbon
148 is considered. Figure 2(c,d) shows the that percent change in C_6 decreases with increasing
149 chain length, using two possible definitions (either the Euclidean length or number of C-C
150 bonds between distal carbon atoms, with the latter yielding a slightly improved correlation).
151 In the context of the particle-in-a-box, a shorter chain, or box, length results in a more
152 loosely-bound excited state, leading to large increases in C_6 upon excitation. Conversely, a
153 longer chain length results in a more-tightly bound excited state, leading to smaller relative
154 increases in C_6 upon excitation. Figure 2(c,d) also shows that C_8 and C_{10} follow the same
155 trends as seen for C_6 , although the percentage increase induced by the excitation is higher

156 for the higher-order dispersion coefficients.

157 Lastly, we decompose the changes in C_6 into contributions from the two types of terms
158 in Equation 2: the moment integrals and atomic polarisabilities. As the densities in the
159 excited states are more diffuse, one might expect that an increase in polarisability would be
160 the primary contribution to the change in molecular C_6 . However, more diffuse densities will
161 also cause a larger average displacement between a reference electron and its corresponding
162 exchange hole, which remains centered near the nearest atomic nucleus.³⁹ Thus the moment
163 integrals also increase upon excitation, and Figure 3 shows that the relative contributions
164 from the moment integrals and polarisabilities are roughly equivalent. This is similar to what
165 is seen for changing chemical environments in ground-state molecules,^{11,13} but contrary to
166 solids where changes in C_6 are dominated by changes in the exchange-hole dipole moment
167 integrals.^{11,14}

168 **B. Push-pull chromophores**

169 Next we consider the set of 4,4'-disubstituted biphenyls shown in Figure 4(a). These
170 molecules can be classified as “push-pull” systems since one substituent is a strong electron-
171 donating group (EDG) while the other is an electron-withdrawing group (EWG). In all
172 cases either the first or second excited state corresponds to a charge-transfer state, as deter-
173 mined from the Hirshfeld charges. In our analysis, the charges and dispersion coefficients of
174 these molecules are partitioned into contributions from the electron-donating and electron-
175 accepting halves which are separated by the central C-C single bond. The extent of charge
176 transfer is determined as the absolute value of the difference in the Hirshfeld charge between
177 the ground and excited state, for either of these two halves of a given molecule.

178 Figure 4(b) shows the extent of charge transfer as a function of the calculated excitation,
179 with both B3LYP and CAM-B3LYP. Range-separated functionals, such as CAM-B3LYP,
180 are conventionally viewed as being the more reliable for charge-transfer excitations,⁵³⁻⁵⁶
181 although one must be careful not to generalise this result, particularly to large systems, as
182 the performance of range-separated functionals is highly system-dependent.⁵⁷⁻⁵⁹ Figure 4(b)
183 shows that going from B3LYP to CAM-B3LYP leads to higher excitation energies and
184 reduced charge transfer, as expected since the latter functional was designed to minimise
185 charge-transfer errors. However, the correlation between these two quantities becomes less

186 clear than with B3LYP. Considering trends with substituent, the amino group is a stronger
187 EDG than the hydroxyl group, resulting in greater charge-transfer and lower excitation
188 energies. For the EWGs, the excitation energies follow the trend $\text{NO}_2 < \text{CHO} < \text{COOH} <$
189 $\text{CN} < \text{CF}_3$ and the extent of charge transfer follows the inverse trend.

190 Figure 4 also shows the change in C_6 for the EDG and EWG halves of the biphenyls,
191 obtained with B3LYP (c) and CAM-B3LYP (d). In general, the C_6 for the EDG decreases
192 upon excitation as charge is transferred away from this region of the molecule, resulting in a
193 more compact electron density. Conversely, the C_6 for the EWG increases upon excitation
194 as charge is transferred to this region of the molecule, resulting in a more diffuse electron
195 density. CAM-B3LYP predicts somewhat lower charge transfer, which results in smaller
196 increases in the EWG C_6 and smaller decreases in the EDG C_6 compared to B3LYP. However,
197 as these effects offset, the overall differences in total C_6 values remain small and are only
198 0-4% for the molecules in the set, with both functionals.

199 Lastly, regarding substituent effects, the magnitude of ΔC_6 for the EDG tends to increase
200 with greater charge transfer, as it becomes more positive in the excited state. For the EWG,
201 the ΔC_6 tends to increase as the extent of charge transfer decreases. This is due to the
202 inverse relationship between charge transfer and excitation energy; reduced charge transfer
203 occurs when the excited state is higher in energy, resulting in more diffuse electron densities
204 and higher C_6 coefficients in the excited state. Additionally, two distinct trends lines are
205 present in Figure 4(c,d), one for each EDG, with larger increases in C_6 occurring for the
206 amino substituent than for the hydroxyl substituent.

207 C. Intermolecular charge-transfer excitations

208 As shown in the previous section, overall increases in molecular dispersion coefficients
209 on excitation are minimal for intramolecular charge-transfer excitations. In this section,
210 we consider two intermolecular charge-transfer complexes: benzene/hexafluorobenzene (in
211 C_{6v} symmetry) and benzene/tetracyanoethylene (in C_{2v} symmetry), both of which possess
212 fairly low-lying intermolecular charge-transfer excitations. Due to the delocalisation (or
213 charge-transfer) error, we expect the results for these intermolecular complexes to be much
214 more sensitive to the choice of density functional than were the data for the biphenyls. We
215 therefore consider the effect of exact-exchange mixing on the extent of excitation-induced

216 charge transfer and changes in the C_6 coefficients using series of hybrid and range-separated
217 hybrid functionals.

218 Figure 5(a,b) show plots of the charge-transfer excitation energy as a function of exact-
219 exchange mixing fraction or range-separation parameter for the two intermolecular com-
220 plexes. In general, the density-functional delocalisation error causes local density functionals
221 (i.e. those with no exact-exchange mixing) to over-stabilise fractional charges and to under-
222 estimate charge-transfer excitation energies^{24–36}. This is reflected in Figure 5(a,b) which
223 show systematic increases in the excitation energies as the exact-exchange mixing fraction
224 or range-separation parameter is increased.

225 Next, Figure 5(c,d) show the excitation-induced charge transfer and reveal differing be-
226 haviour for these complexes. In both cases, the BLYP functional, with no exact-exchange
227 mixing, predicts fractional charge transfer of near one-half of an electron ($0.58 e^-$ for ben-
228 zene/hexafluorobenzene and $0.44 e^-$ for benzene/tetracyanoethylene). This is expected as
229 delocalisation error causes local functionals to over-stabilise fractional charges. As exact
230 exchange is incorporated into the functional, the extent of charge transfer tends towards
231 integer values. However, the trends are opposing for the complexes, with the charge trans-
232 fer decreasing to zero for benzene/hexafluorobenzene and increasing to $0.8 e^-$ for ben-
233 zene/tetracyanoethylene. This would seem to imply that the latter case is a “true” charge-
234 transfer excitation, while the low-energy charge-transfer excitation seen in the former com-
235 plex is an artifact caused by delocalisation error.

236 Finally, Figure 5(e,f) show the excitation-induced changes in C_6 London dispersion coeffi-
237 cients for the complexes, as well as for the component donor and acceptor molecules. Despite
238 the high sensitivity of both the charges and excitation energies, the dispersion coefficients
239 show minimal functional dependence, particularly for benzene/tetracyanoethylene. This in-
240 dicates that use of popular hybrid functionals, like B3LYP, should be adequate to describe
241 dispersion properties, even for strong charge-transfer excitations. As for the disubstituted
242 biphenyls, the C_6 of the electron donor decreases on excitation while the C_6 of the electron
243 acceptor increases. These effects offset almost completely for benzene/tetracyanoethylene;
244 however, for benzene/hexafluorobenzene, there is a net increase in C_6 of roughly 10%, much
245 larger than those seen in the biphenyls or conjugated hydrocarbons. This implies that
246 changes in dispersion energy coming from excitation may be larger for co-crystals than
247 single-molecule crystals, and this will be confirmed in the following section.

248 D. Dispersion in crystalline solids

249 Having established that electronic excitation has the potential to cause large changes in
250 molecular dispersion coefficients, we next assess the impact of this effect on the dispersion
251 energy for interaction of a single molecule with a surrounding crystal environment. We
252 consider a set of 4 single-molecule crystals and 6 co-crystals, shown in Figure 6.

253 The results in Table I show that the changes in C_6 on excitation remain quite low for the
254 single molecules exhibiting intramolecular charge-transfer excitations, as expected from the
255 results in Section III B. While $\% \Delta C_6$ may be significantly larger in magnitude for some of
256 the intermolecular charge-transfer excitations, the resulting changes in dispersion energy for
257 excitation of a molecular dimer within the co-crystal remain quite small in magnitude. This
258 is partly because the moment integrals and polarisabilities for only a single molecular dimer
259 are changing, so the resulting effect on the dispersion coefficients for interactions with the
260 remainder of the crystal are effectively halved relative to what would be seen for interaction
261 between two excited moieties. Additionally, the larger relative increases in the higher-order
262 dispersion coefficients (Figure 1) cause increases in the effective atomic van der Waals radii
263 used in the XDM damping function. This results in increased damping of the dispersion
264 energy, which largely offsets the effect of increasing dispersion coefficients. Indeed, in the
265 majority of cases considered, the increased damping causes a lower dispersion energy in the
266 excited state than in the ground state, as reflected by the many positive values of ΔE_{disp} in
267 Table I.

268 The largest changes in dispersion energy resulting from a localised excitation are -1.2
269 kcal/mol for benzene/hexafluorobenzene and 1.2 kcal/mol for naphthalene/hexafluorobenzene.
270 While examples could likely be found with larger dispersion-energy changes, this finding
271 indicates that this dispersion effect has a very minor contribution to the overall excitation
272 energy for a molecule or dimer in the condensed phase.

273 IV. SUMMARY

274 This is the first work to consider the effect of electronic excitation on molecular London
275 dispersion coefficients. Excitation increases the dispersion coefficients as the electron density
276 distribution in the excited state is more diffuse, resulting in larger atomic polarisabilities

277 and exchange-hole multipole moment integrals, with these two contributions being roughly
278 equivalent in size. The percentage change in the C_6 dispersion coefficient was found to
279 decrease with increasing chain length for $\pi \rightarrow \pi^*$ excitations in conjugated hydrocarbons.
280 For charge-transfer excitations, the dispersion coefficients for the electron-donating moiety
281 decrease, while the dispersion coefficients for the electron-withdrawing moiety increase. The
282 combined effect on the overall dispersion coefficient is negligible for intramolecular charge
283 transfer, but can be fairly large for intermolecular charge transfer. However, despite the
284 potential for large changes in dispersion coefficients, electronic excitation of a single molecule
285 has only a minimal effect on the dispersion energy for interaction of the chromophore with
286 the surrounding bulk in a molecular crystal or co-crystal.

287 V. ACKNOWLEDGEMENTS

288 The authors thank the Natural Sciences and Engineering Research Council of Canada
289 (NSERC) for financial support (E.R.J.) and Compute Canada (ACEnet and Westgrid), for
290 computational time. We also thank Dr. Stephen G. Dale for helpful discussions.

291 REFERENCES

- 292 ¹Y. Yang, B. Rice, X. Shi, J. R. Brandt, R. Correa da Costa, G. J. Hedley, D.-M. Smilgies,
293 J. M. Frost, I. D. W. Samuel, A. Otero-de-la-Roza, E. R. Johnson, K. E. Jelfs, J. Nelson,
294 A. J. Campbell, and M. J. Fuchter, *ACS Nano* **11**, 8329 (2017).
295 ²M. K. Ravva, A. Risko, and J.-L. Brédas, in *Non-covalent Interactions in Quantum*
296 *Chemistry and Physics*, edited by A. Otero-de-la Roza and G. A. DiLabio (Elsevier, 2017)
297 Chap. 9, pp. 277–302.
298 ³W. Barford, N. Paiboonvorachat, and D. Yaron, *J. Chem. Phys.* **134**, 234101 (2011).
299 ⁴C. Amovilli and F. M. Floris, *J. Phys. Chem. A* **119**, 5327 (2015).
300 ⁵Y. Iwabata and H. Nakai, *J. Chem. Phys.* **137**, 124106 (2012).
301 ⁶A. D. Laurent, C. Adamo, and D. Jacquemin, *Phys. Chem. Chem. Phys.* **16**, 14334 (2014).
302 ⁷S. Grimme, *J. Comput. Chem.* **27**, 1787 (2006).
303 ⁸S. Grimme, J. Antony, S. Ehrlich, and H. Krieg, *J. Chem. Phys.* **132**, 154104 (2010).
304 ⁹A. D. Becke and E. R. Johnson, *J. Chem. Phys.* **127**, 154108 (2007).

305 ¹⁰A. Otero-de-la Roza and E. R. Johnson, *J. Chem. Phys.* **138**, 204109 (2013).

306 ¹¹E. R. Johnson, in *Non-covalent Interactions in Quantum Chemistry and Physics*, edited
307 by A. Otero-de-la Roza and G. A. DiLabio (Elsevier, 2017) Chap. 5, pp. 169–194.

308 ¹²A. Otero-de-la Roza and E. R. Johnson, *J. Chem. Phys.* **138**, 054103 (2013).

309 ¹³E. R. Johnson, *J. Chem. Phys.* **135**, 234109 (2011).

310 ¹⁴M. S. Christian, A. Otero-de-la-Roza, and E. R. Johnson, *J. Chem. Theory Comput.* **12**,
311 3305 (2016).

312 ¹⁵M. Mohebifar, E. R. Johnson, and C. N. Rowley, *J. Chem. Theory Comput.* (2017),
313 submitted.

314 ¹⁶M. J. Frisch, G. W. Trucks, H. B. Schlegel, G. E. Scuseria, M. A. Robb, J. R. Cheese-
315 man, G. Scalmani, V. Barone, B. Mennucci, G. A. Petersson, H. Nakatsuji, M. Caricato,
316 X. Li, H. P. Hratchian, A. F. Izmaylov, J. Bloino, G. Zheng, J. L. Sonnenberg, M. Hada,
317 M. Ehara, K. Toyota, R. Fukuda, J. Hasegawa, M. Ishida, T. Nakajima, Y. Honda, O. Ki-
318 tao, H. Nakai, T. Vreven, J. A. Montgomery, Jr., J. E. Peralta, F. Ogliaro, M. Bearpark,
319 J. J. Heyd, E. Brothers, K. N. Kudin, V. N. Staroverov, R. Kobayashi, J. Normand,
320 K. Raghavachari, A. Rendell, J. C. Burant, S. S. Iyengar, J. Tomasi, M. Cossi, N. Rega,
321 J. M. Millam, M. Klene, J. E. Knox, J. B. Cross, V. Bakken, C. Adamo, J. Jaramillo,
322 R. Gomperts, R. E. Stratmann, O. Yazyev, A. J. Austin, R. Cammi, C. Pomelli, J. W.
323 Ochterski, R. L. Martin, K. Morokuma, V. G. Zakrzewski, G. A. Voth, P. Salvador,
324 J. J. Dannenberg, S. Dapprich, A. D. Daniels, O. Farkas, J. B. Foresman, J. V. Ortiz,
325 J. Cioslowski, and D. J. Fox, “Gaussian 09 Revision A.1,” Gaussian Inc. Wallingford CT
326 2009.

327 ¹⁷A. D. Becke, *J. Chem. Phys.* **98**, 5648 (1993).

328 ¹⁸C. Lee, W. Yang, and R. G. Parr, *Phys. Rev. B* **37**, 785 (1988).

329 ¹⁹M. E. Casida, in *Recent Advances in Density Functional Methods, Vol 1*, edited by D. P.
330 Chong (World Scientific, Singapore, 1995) Chap. 5, pp. 155–192.

331 ²⁰R. Bauernschmitt and R. Ahlrichs, *Chem. Phys. Lett.* **256**, 454 (1996).

332 ²¹R. E. Stratmann, G. E. Scuseria, and M. J. Frisch, *J. Chem. Phys.* **109**, 8218 (1998).

333 ²²C. Adamo and D. Jacquemin, *Chem. Soc. Rev.* **42**, 845 (2013).

334 ²³T. Yanai, D. P. Tew, and N. C. Handy, *Chem. Phys. Lett.* **393**, 51 (2004).

335 ²⁴D. J. Tozer, R. D. Amos, N. C. Handy, B. O. Roos, and L. Serrano-Andrès, *Mol. Phys.*
336 **97**, 859 (1999).

337 ²⁵Z.-L. Cai, K. Sendt, and J. R. Reimers, *J. Chem. Phys.* **117**, 5543 (2002).

338 ²⁶A. Dreuw, J. L. Weisman, and M. Head-Gordon, *J. Chem. Phys.* **119**, 2943 (2003).

339 ²⁷D. J. Tozer, *J. Chem. Phys.* **119**, 12697 (2003).

340 ²⁸O. Gritsenko and E. J. Jan Baerends, *J. Chem. Phys.* **121**, 655 (2004).

341 ²⁹G. Sini, J. S. Sears, and J.-L. Bredas, *J. Chem. Theory Comput.* **7**, 602 (2011).

342 ³⁰S. N. Steinmann, C. Piemontesi, A. Delacht, and C. Corminboeuf, *J. Chem. Theory*
343 *Comput.* **8**, 1629 (2012).

344 ³¹E. Ruiz, D. R. Salahub, and A. Vela, *J. Phys. Chem.* **100**, 12265 (1996).

345 ³²A. Ruzsinszky, J. P. Perdew, G. I. Csonka, O. A. Vydrov, and G. E. Scuseria, *J. Chem.*
346 *Phys.* **125**, 194112 (2006).

347 ³³A. J. Cohen, P. Mori-Sánchez, and W. Yang, *Science* **321**, 792 (2008).

348 ³⁴M.-C. Kim, E. Sim, and K. Burke, *Phys. Rev. Lett.* **111**, 073003 (2013).

349 ³⁵E. R. Johnson, A. Otero de la Roza, and S. G. Dale, *J. Chem. Phys.* **139**, 184116 (2013).

350 ³⁶A. D. Becke, *J. Chem. Phys.* **140**, 18A301 (2014).

351 ³⁷A. D. Becke, *Phys. Rev. A* **38**, 3098 (1988).

352 ³⁸H. Iikura, T. Tsuneda, T. Yanai, and K. Hirao, *J. Chem. Phys.* **115**, 3540 (2001).

353 ³⁹A. Becke and M. Roussel, *Phys. Rev. A* **39**, 3761 (1989).

354 ⁴⁰E. I. Sánchez-Flores, R. Chávez-Calvillo, T. A. Keith, G. Cuevas, T. Rocha-Rinza, and
355 F. Cortés-Guzmán, *J. Comp. Chem.* **35**, 820 (2014).

356 ⁴¹R. Bauernschmitt and R. Ahlrichs, .

357 ⁴²M. E. Casida and T. A. Wesolowski, *Int. J. Quantum Chem.* **96**, 577 (2004).

358 ⁴³A. D. Becke and E. R. Johnson, *J. Chem. Phys.* **123**, 154101 (2005).

359 ⁴⁴The postg program can be downloaded from <http://schooner.chem.dal.ca>.

360 ⁴⁵F. L. Hirshfeld, *Theor. Chim. Acta* **44**, 129 (1977).

361 ⁴⁶T. Han, Y. Hong, N. Xie, S. Chen, N. Zhao, E. Zhao, J. W. Y. Lam, H. H. Y. Sung,
362 Y. Dong, B. Tong, and B. Z. Tang, *J. Mater. Chem. C* **1**, 7314 (2013).

363 ⁴⁷F. H. Allen, *Acta Cryst. B* **58**, 380 (2002), crystal structures can be obtained free of charge
364 via http://www.ccdc.cam.ac.uk/data_request/cif.

365 ⁴⁸A. Becke, *J. Chem. Phys.* **85**, 7184 (1986).

366 ⁴⁹J. P. Perdew, K. Burke, and M. Ernzerhof, *Phys. Rev. Lett.* **77**, 3865 (1996).

367 ⁵⁰A. Otero-de-la Roza and E. R. Johnson, *J. Chem. Phys.* **136**, 174109 (2012).

- 368 ⁵¹P. Giannozzi, S. Baroni, N. Bonini, M. Calandra, R. Car, C. Cavazzoni, D. Ceresoli,
369 G. Chiarotti, M. Cococcioni, I. Dabo, *et al.*, J. Phys.: Condens. Matter **21**, 395502 (2009).
- 370 ⁵²A. Otero-de-la Roza, E. R. Johnson, and V. Luaña, Comput. Phys. Commun. **185**, 1007
371 (2014).
- 372 ⁵³A. Dreuw and M. Head-Gordon, J. Am. Chem. Soc. **126**, 4007 (2004).
- 373 ⁵⁴M. J. G. Peach, P. Benfield, T. Helgaker, and D. J. Tozer, J. Chem. Phys. **128**, 044118
374 (2008).
- 375 ⁵⁵K. A. Nguyen, R. Ruth Pachter, and P. N. Day, J. Chem. Phys. **140**, 244101 (2014).
- 376 ⁵⁶A. D. Laurent and D. Jacquemin, Int. J. Quantum Chem. **113**, 2019 (2013).
- 377 ⁵⁷T. Koerzdoerfer, J. S. Sears, C. Sutton, and J. L. Bredas, J. Chem. Phys. **135**, 204107
378 (2011).
- 379 ⁵⁸S. R. Whittleton, X. A. S. Vazquez, C. M. Isborn, and E. R. Johnson, J. Chem. Phys.
380 **142**, 184106 (2015).
- 381 ⁵⁹K. Garrett, X. A. Sosa Vazquez, S. B. Egri, J. Wilmer, L. E. Johnson, B. H. Robinson,
382 and C. M. Isborn, J. Chem. Theory Comput **10**, 3821 (2014).

TABLE I: Changes in molecular C_6 coefficients for a single excited moiety (single molecule or charge-transfer dimer) and overall dispersion energies for interaction of the chromophore with surrounding molecules in the crystal.

Molecule	$\% \Delta C_6$	ΔE_{disp} (kcal/mol)
4-amino-4'-nitrobiphenyl	0.3	-0.16
A3MN	0.9	0.17
coumarin	1.9	0.18
6-aminocoumarin	2.8	0.14
benzene/hexafluorobenzene	7.8	-1.24
N,N-dimethylaniline/hexafluorobenzene	2.8	0.07
naphthalene/hexafluorobenzene	4.6	1.23
tetracyanoethylene/naphthalene	-0.3	0.39
chloranilic acid/pyrazine	-0.3	0.46
2,5-dimethylbenzoquinone/bis(hydroquinone)	24.4	1.02

FIG. 1: The constituents of conjugated-chain set of molecules.

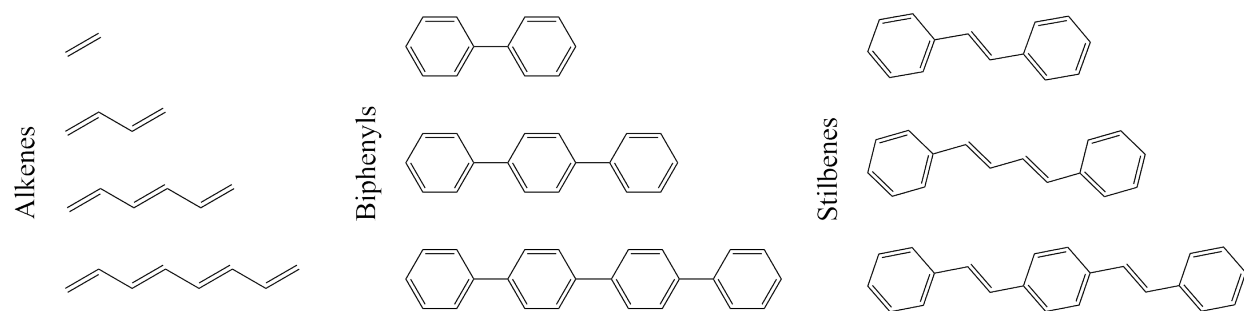


FIG. 2: Changes in molecular C_6 dispersion coefficients as a function of excitation energy for subsets of (a) alkenes and (b) stilbenes and biphenyls. Also shown are changes in C_6 , C_8 , and C_{10} dispersion coefficients for the conjugated-chain set as a function of chain length using two different definitions: (c) the Euclidean distance between terminal carbon atoms and (d) the number of C-C bonds forming the chain. The lines are to guide the eye.

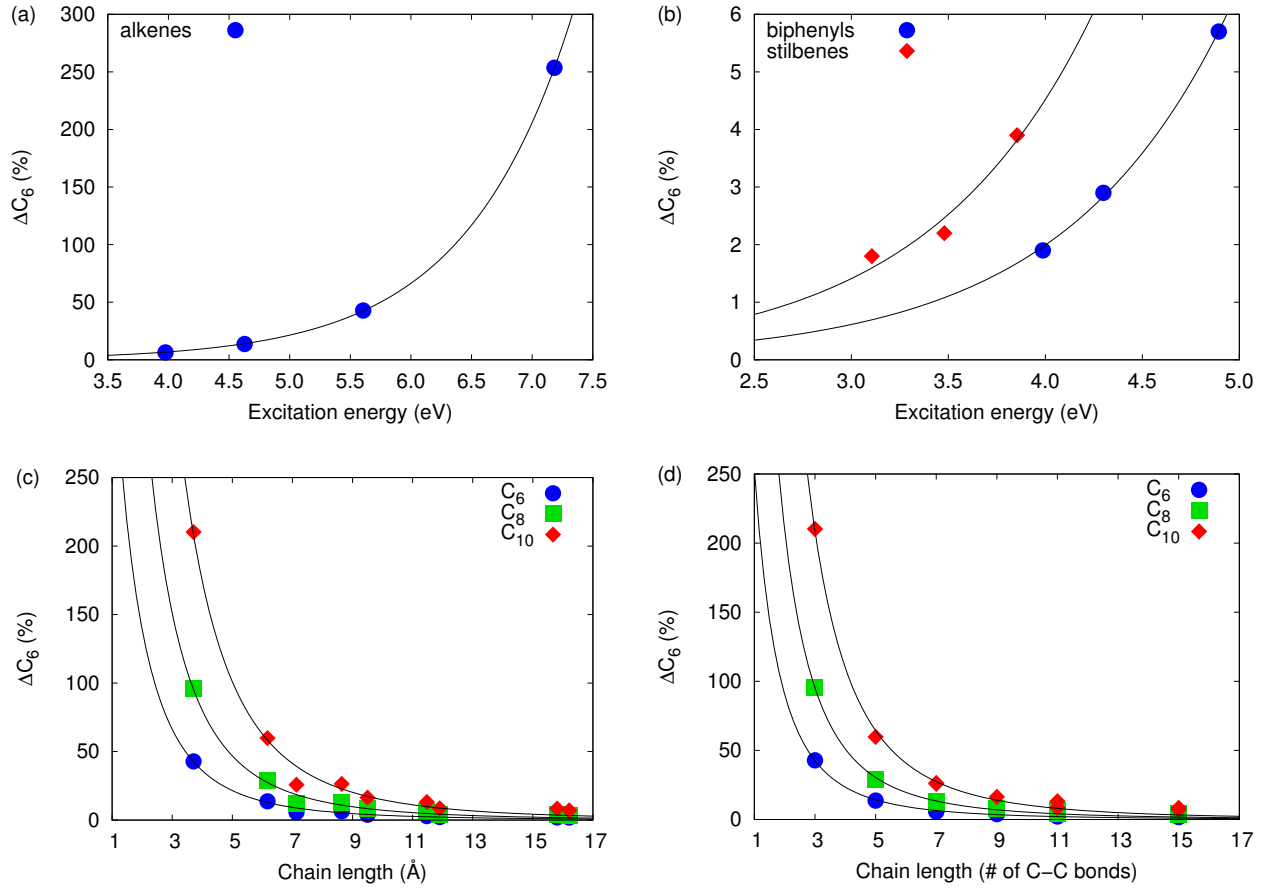


FIG. 3: Decomposition of the changes in molecular C_6 dispersion coefficients into contributions from the dipole-moment integrals and polarisabilities. Results are shown for the conjugated-chain set as a function of chain length, defined as the number of C-C bonds forming the chain.

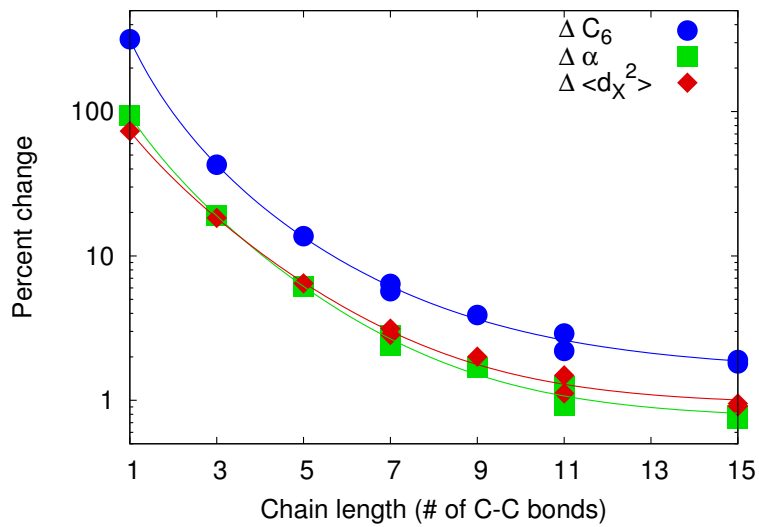


FIG. 4: The set of selected 4,4'-disubstituted biphenyls (a) together with the calculated extent of charge transfer as a function of excitation energy (b). Also shown are the excitation-induced changes in C_6 for the electron-donating and electron-withdrawing halves of each biphenyl from B3LYP (c) and CAM-B3LYP (d). Coloured symbols correspond to hydroxyl electron donors and open symbols correspond to amino electron donors.

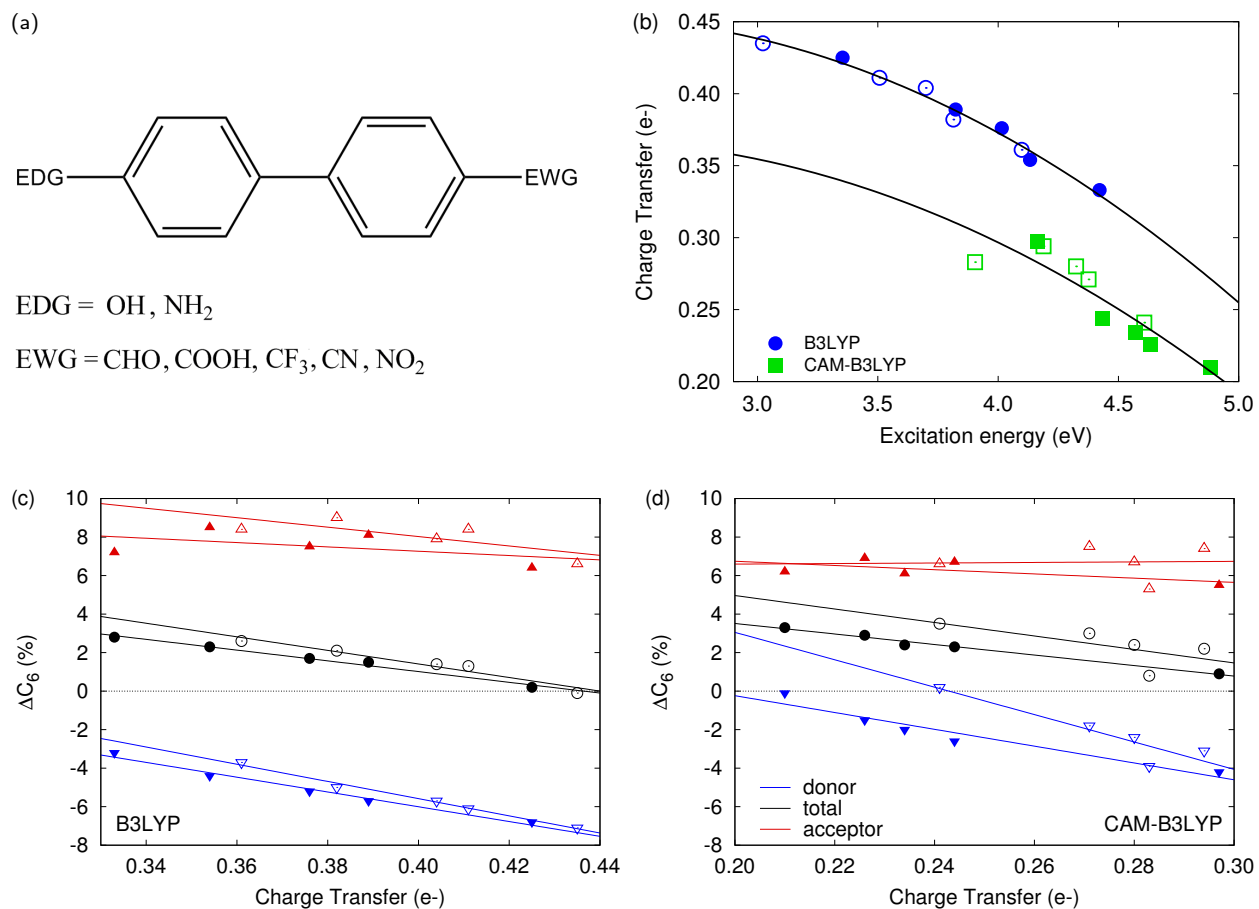


FIG. 5: Calculated properties of the benzene/hexafluorobenzene (left) and benzene/tetracyanoethylene (right) complexes as a function of exact-exchange mixing (a_X) in BLYP-based hybrids (filled symbols, solid lines) or range-separation (ω) parameters in LC-BLYP-based functionals (open symbols, dashed lines). Shown are the excitation energies (top row), extent of excitation-induced charge transfer (middle row), and excitation-induced changes in C_6 dispersion coefficients (bottom row).

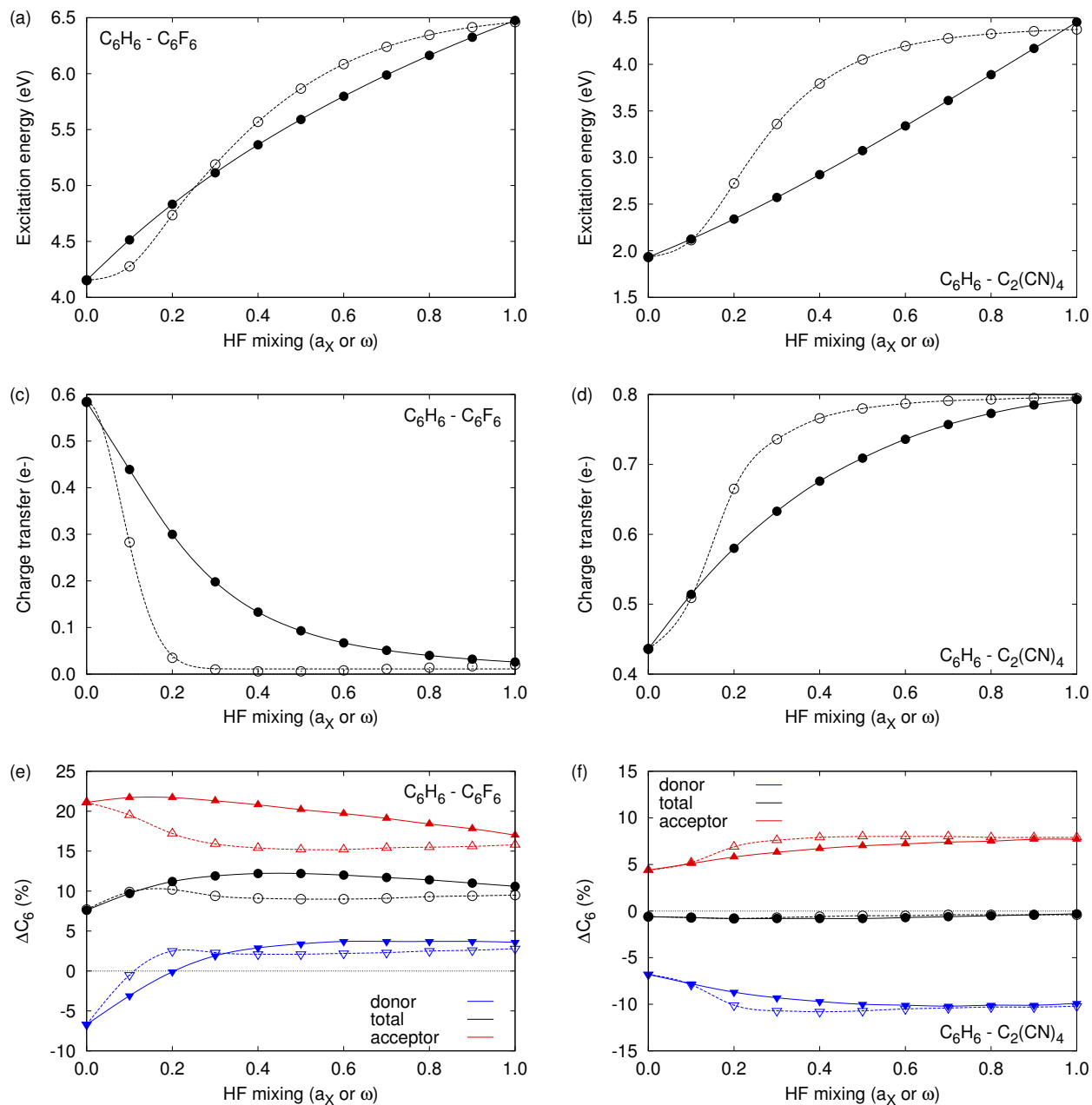


FIG. 6: Structures of selected chromophores present in molecular crystals together with their CCDC codes.

